

# Effect of aluminum oxide nanoparticles on the rheology and stability of a biopolymer for enhanced oil recovery.

ORODU, K.B., AFOLABI, R.O., OLUWASIJUWOMI, T.D., ORODU, O.D.

2019



1 **Title:** Effect of Aluminum Oxide Nanoparticles on the Rheology and Stability of a Biopolymer  
2 for Enhanced Oil Recovery

3 **Authors:** Kale B. Orodu<sup>1</sup>, Richard O. Afolabi<sup>1,2</sup>, Toyosi D. Oluwasijuwomi<sup>1</sup>, Oyinkepreye D.  
4 Orodu<sup>1\*</sup>

5 **Affiliations:**

6 <sup>1</sup>Department of Petroleum Engineering, Covenant University, Ota, Ogun State, Nigeria.

7 <sup>2</sup>Robert Gordon University, Aberdeen, UK.  
8

9 **\*Contact email:** oyinkepreye.orodu@covenantuniversity.edu.ng; preye.d.orodu@gmail.com

10 **Abstract**

11 Uncommon and untested biopolymers in field pilot studies, but applied in laboratory studies  
12 are combined with Al<sub>2</sub>O<sub>3</sub> nanoparticles to form nanocomposites for enhanced oil recovery  
13 (EOR) performance evaluation. Core plug samples of the Niger Delta region and Berea  
14 sandstone were used as the porous media for EOR experiments. Incremental oil recovery sequel  
15 to waterflooding (secondary recovery) was 5 – 12 % and 5 – 7% for potato starch  
16 nanocomposite (PSPNP) and gum arabic nanocomposite (GCNP) respectively. The  
17 biopolymer nanocomposites showed improved viscosity over the biopolymers. Thus, the  
18 nanoparticle served as a viscosity modifier on one-hand and stability enhancer on the other.  
19 EOR was affected by biopolymer and nanoparticle concentration with the attendant catch-22  
20 situation of permeability impairment. The overall higher incremental recovery of applying  
21 PSPNP came by an intermediate potato starch (PSP) flooding between waterflooding and  
22 PSNP flooding. Consequently, slugs of biopolymer and biopolymer nanocomposite may be the  
23 way forward knowing that the biopolymers studied have surface-active constituents.  
24

25 **Keywords:** Enhanced Oil Recovery, Biopolymers, Nanoparticles, Rheology  
26  
27

28 **1. Introduction**

29 Enhanced oil recovery (EOR) schemes otherwise referred to as tertiary recovery has been  
30 applied to go the extra mile of improving oil recovery (Hendraningrat *et al.*, 2013a; Li *et al.*,  
31 2013). This sees recovery going beyond the primary means of the reservoir's in-situ energy,  
32 and secondary recovery that is commonly exploited by water and immiscible gas flooding.  
33 Recent research, albeit confined to laboratory scale testing for the oil and gas industry goes the  
34 way of innovative worldwide application of nanotechnology and miniaturised devices (Maghzi  
35 *et al.*, 2012; Roustaei *et al.*, 2012; Osamah *et al.*, 2015). The focus is now on functionalized  
36 nanoparticles for the control of matter at the nanoscale level (Hendraningrat *et al.*, 2013b; Sun  
37 *et al.*, 2017). Nanoparticle retention has been a subject for concern. Nanoparticle adsorption  
38 onto solid surfaces may impede nanoparticle transport even for nanoparticles of appropriate  
39 size, shape, and good stability (Rodriguez *et al.*, 2009). Adsorption of nanoparticles mainly  
40 takes place due to interactions of chemicals and rock surfaces through hydrogen bonding,  
41 hydrophobic bonding, and covalent bonding (Hendraningrat *et al.*, 2013a; Hendraningrat *et al.*,  
42 2013b). There is a need to prevent these interactions by changing some occurring phenomenon  
43 in the system. This has necessitated the use of polymer-coated nanoparticles. The polymer  
44 flooding technology for EOR can be classified as a proven technology due to its wide field  
45 application in recent years (Abidin *et al.*, 2012). Hydrolyzed Polyacrylamide (HPAM) and

46 Carboxyl Methyl Cellulose (CMC) have been used over the years in the displacement of crude  
47 oil from reservoirs. The use of polymers in flooding operations is to reduce mobility when  
48 dissolved in water (Abidin *et al.*, 2012; Yousefvand and Jafari, 2015). The increase in viscosity  
49 is responsible for the reduction in oil/water mobility ratio. This is achieved by an increase in  
50 the polymer concentration in aqueous solution (Yu *et al.*, 2010; Ogolo *et al.*, 2012;  
51 ShamsiJazeyi *et al.*, 2014). HPAM is the most widely used polymer for EOR operations, and  
52 this is due to its low price and good rheological properties. Furthermore, the procedure for  
53 implementing EOR schemes involving the use of HPAM is less difficult, and oil recovery is  
54 significantly improved under standard reservoir conditions (Abidin *et al.*, 2012). However,  
55 there are limitations to the increment in the concentrations of the polymers. It has been reported  
56 that increment of more than 10% in the case of CMC adversely affects the displacement of oil  
57 (Abidin *et al.*, 2012). Furthermore, CMC becomes poorly miscible with water at concentrations  
58 greater than 10% thereby making the injection into reservoirs difficult. The use of HPAM has  
59 its drawbacks as well; with reported cases of degradation under high temperature (usually  
60 above 99 °C depending on brine hardness) and sensitivity to salinity, precipitation occurs if  
61 Ca<sup>2+</sup> and Mg<sup>2+</sup> are present (Abidin *et al.*, 2012; Lewandowska, 2006). However, the recent  
62 study on HPAM-based silica nanocomposite has brought improvement on HPAM application  
63 in high temperature and high salinity environment (Hu *et al.*, 2017). The use of biopolymers  
64 such as xanthan gum has proven to perform well in high salinity brine and compatible with  
65 most injected fluid additives for EOR operations. Besides its salinity resistance, new techniques  
66 have been reported which improves the thermal stability of biopolymers up to 105°C.  
67 Moreover, such polymers produced as either broth or concentrate form can be made to working  
68 concentrations without the need for elaborate shear mixing equipment. Advancement in  
69 nanotechnology has shown that the use of nanoparticles in polymer flooding operations can  
70 increase the oil recovery factor (Yousefvand and Jafari, 2015; Saha *et al.*, 2018). There exist a  
71 few pieces of research about biopolymer performances in the presence of nanoparticles (Abidin  
72 *et al.*, 2012; ShamsiJazeyi *et al.*, 2014) for enhanced oil recovery. In this work, the effect of  
73 alumina nanoparticles on oil recovery during polymer flooding by biopolymers is investigated.  
74 The biopolymers considered include the naturally occurring Gum Arabic and an experimentally  
75 derived biopolymer from potatoes peels. The rheology of the polymer nanocomposite was  
76 investigated under high temperature and salinity.

## 77 2. Materials and Method

### 78 2.1. Materials

79 Laboratory grade Sodium Chloride [NaCl] was used to prepare brine and Acetone [C<sub>3</sub>H<sub>6</sub>O] for  
80 core cleaning. Core plugs of the Offshore Depobelt – Niger Delta (Niger Delta consist of five  
81 depobelts which are Northern, Greater Ughelli, Coastal Swamp 1 & 2 and Offshore) were  
82 acquired for core flooding. Also, Berea sandstone cores were purchased from Cleveland  
83 Quarries Inc. Other materials are crude oil of 34.97 °API from the Niger Delta (Izombe Oilfield,  
84 OML 124), Polymer (Gum Arabic), Al<sub>2</sub>O<sub>3</sub> (30-60 nm, purity greater than 99 %; manufactured  
85 by Sigma Aldrich and purchased from Equilab Solutions in Nigeria), Gum Arabic polymer and  
86 potato peels. Potatoes used were purchased at Ota, Nigeria (7.95°N, 4.783°E) and Gum Arabic  
87 from Kaduna, Nigeria (10° 31' 23" N, 7° 26' 25" N). Deionised water was used as the base fluid  
88 for nanoparticle and polymer to formulate nanofluid and polymer solutions respectively.  
89 The equipment used for core flooding and viscosity is OFITE®'s reservoir permeability tester  
90 (RPT) and OFITE®'s direct indicator viscometer (8-speed). Other equipment includes Vinci  
91 Equipment's high-pressure core saturator (used for initial saturation of core plugs with brine),  
92 pycnometer (used for measuring crude oil density), desiccator (used for storing cleaned and  
93 dried cores), Soxhlet apparatus (used for cleaning the cores of crude oil and formation brine)  
94 etc.

95

### 96 2.1.1 Potato Starch

97 Potato starch forms paste having high viscosity. The high viscosity endears it as a possible  
98 agent for enhanced oil recovery since the mobility ratio of the displacement process is reduced.  
99 Other properties are its binding capacity and formation of gel within 50 – 80 °C (Herrera *et al.*,  
100 2017; LeCorre *et al.*, 2012). The gelatinisation temperature has and can be modified (Oosten,  
101 1982) to ensure its use within the confines of petroleum reservoir temperature. Potato starch  
102 contains amylose and amylopectin. Minor components include protein and lipids in relatively  
103 small amounts. The most common application of starch is in the food industry just like gum  
104 arabic.

105 Weight averaged molecular (Mwt) and standard deviation (SD) of a typical native starch for  
106 potato is 2.305E-06 g/mol and 0.004E-06 respectively (Bidzinska *et al.*, 2015). The Mwt from  
107 potato starch peel used in this study was not measured, it is noted that there are merits and  
108 demerits of various techniques available for the measurement of the Mwt of starch (Harding *et*  
109 *al.*, 2016). Furthermore, it is essential to note that any two starch that has the same Mwt and  
110 different SD will have different rheological properties (Gilbert *et al.*, 2010).

111

### 112 2.1.2 Gum Arabic

113 Gum Arabic (GA) is a gum exudate produced by *Acacia senegal* and *Acacia seyal* trees. It is  
114 known as an emulsifying agent for the food industry primarily. The constituents are mainly  
115 arabinogalactan (AG), arabinogalactan protein (AGP) and glycoprotein (GP) in the average  
116 proportions of  $\approx 90\%$ ,  $\approx 10\%$ , and  $\approx 1\%$  (Mahendran *et al.*, 2008; Renard *et al.*, 2006). The  
117 molecular structure and composition of GA and its biophysical properties of *Acacia Senegal*  
118 from Nigeria were investigated by Gashua (2016). Transmission electron microscopy (TEM)  
119 analysis showed varied macromolecules of size from 12 to 60 nm (Tan, 2004). The properties  
120 of GA endearing its use in the food industry are due to the emulsification, microencapsulation,  
121 thickening and stabilisation capability. AGP fraction of GA possess the emulsifying property,  
122 and GA is soluble in water. This capability is contributed to by the hydrophilic sugar residues  
123 and the hydrophobic amino acids and so latches on to the oil-water interface (Degean *et al.*,  
124 2012). These substances are the hydrophilic polysaccharide (sugar residues) and hydrophobic  
125 polypeptide chains (Buffo *et al.*, 2001)

126

## 127 2.2. Polymer and Polymer-Nanocomposite Preparation

128 The starch used in the biopolymer preparation was extracted from the potato peel. 120 g of  
129 potato peel was washed and grated into smaller sizes. The grated potato peels were added to  
130 350 ml of water after which it was blended for 15 minutes. The blended potato peels were  
131 sieved leaving the larger sizes of potato starch behind. The sieved mixture was allowed to settle  
132 for 8 hours. The settled mixture was decanted to obtain the starch at the bottom of the mixture.  
133 The obtained starch was air dried for 20 hours to remove any form of moisture present.

134 Starch polymer preparation involves: (a) distilled water added to starch at specific  
135 concentration and (b) pre-gelatinised starch prepared by slowly heat solution to 60 °C with  
136 continuous stirring made possible by a magnetic stirrer.

137 Gum Arabic (GA) solution was prepared with deionised and then aged for 5 days at room  
138 temperature. Al<sub>2</sub>O<sub>3</sub> nanofluid was likewise prepared with deionised water. GANanocomposite  
139 (GCNP) came up by blending to give 3 wt% GA and 1.33 wt% Al<sub>2</sub>O<sub>3</sub>, and 5 wt% GA and 1.33  
140 wt% Al<sub>2</sub>O<sub>3</sub> solution. Similarly, Potato Peel Starch Polymer Nanocomposite (PSPNP) of 5 wt%  
141 potato starch (PSP) and 0.5 wt% Al<sub>2</sub>O<sub>3</sub>, 5 wt% PSP and 1.0 wt% Al<sub>2</sub>O<sub>3</sub>, 5 wt% PSP and 1.5

142 wt% Al<sub>2</sub>O<sub>3</sub> respectively. Also, the solutions for PSPNP were generated at two saline  
 143 concentrations of 2.5 wt% and 5.0 wt%. The choice of polymer concentration of Gum Arabic  
 144 and Potato Starch arose from the works of Taiwo and Olafuyi (2015) with the use of 5 wt%  
 145 GA polymer slug. Other considerations were interfacial tension (IFT) reduction by polymeric  
 146 nanofluid with nanoparticle concentration of 1.5 wt% and 2.0 wt%/v (Maurya *et al.*, 2017;  
 147 Sharma and Sangwai, 2017) and wettability alteration based on an optimal nanoparticle  
 148 concentration of 2 – 3 wt% (Ju and Fan, 2009).

149  
 150 *2.3. Rheology*

151 Measurement of parameters for the computation of viscosity in base on the tabulated process  
 152 in Table 1

**Table 1** – Scheme for Measurement of Rheological Properties

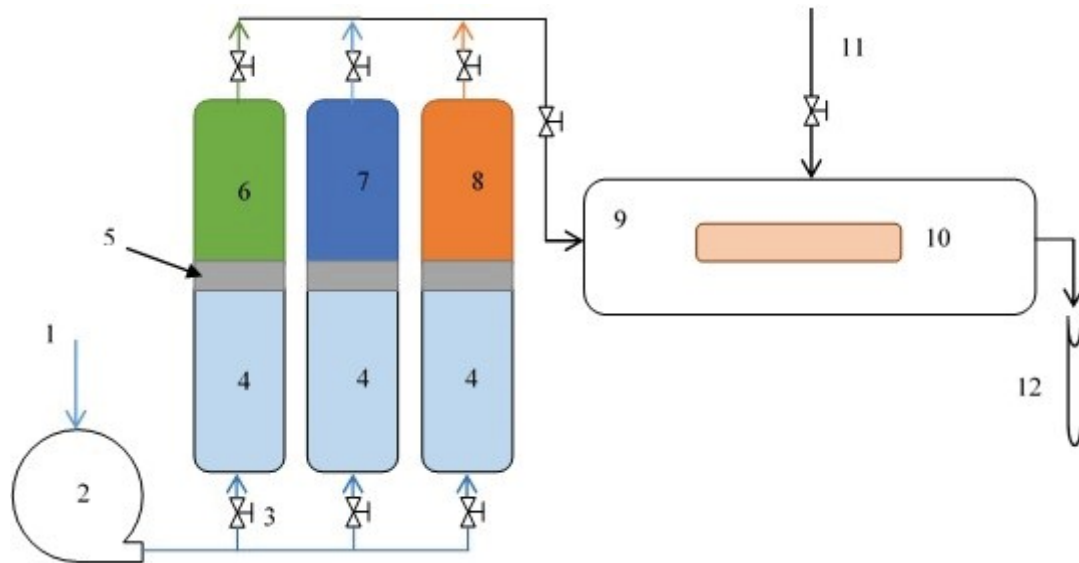
S/N	Experiment	Starch	Gum Arabic
1.	Aging of the polymer at ambient condition	≈ 48 hrs	24 hrs
2.	Heating of polymer and intermittent stirring before Viscosity measurement (dial reading at each speed) *different polymer blend for each speed	15 – 20 mins	5 – 10 mins
3.	Stable dial reading	2 mins	2 mins

155  
 156 At each temperature of 50 °C, 100 °C, and 150 °C, the sample polymer (and polymer  
 157 nanocomposite) was heated 10 °C above the specified temperature as the measurement of  
 158 viscosity was not done simultaneously with heating the polymer.

159  
 160 *2.4. Experimental Core Flooding*

161 Core samples were cleaned with acetone in a Soxhlet apparatus to remove oil and existing salt  
 162 and dried in an oven at a controlled temperature, followed by being stored in a desiccator. The  
 163 samples were weighed and saturated with prepared brine (3 wt.%) by the use of a saturator for  
 164 computation of porosity and pore volume. Fluid density and viscosity were measured with  
 165 pycnometer and glass capillary viscometer. Core flooding was conducted with OFITE's  
 166 Reservoir Permeability Tester (RPT). The schematic of the coreflood setup is as shown in  
 167 Figure 1. All flooding experiments were performed at ambient condition, and the differential  
 168 pressure was measured across the core holder. The core flooding scheme progressed by the  
 169 initial saturation of core at 3 wt.% brine. This is a primary imbibition process followed  
 170 sequentially by a drainage process to displace the brine. Oil was used to displace the brine at a  
 171 specific rate until no brine was produced anymore.

172



173

174 **Figure 1** – Schematic of the core flooding apparatus (OFITE reservoir permeability tester). 1)  
 175 fluid supply, 2) 515 HPLC pump, 3) valves, 4) water, 5) drive piston, 6) crude oil, 7) brine, 8)  
 176 polymer or nanocomposite, 9) Hassler cell holder, 10) core plug, 11) confining pressure, 12)  
 177 test tube for effluent.

178

179 The primary drainage procedure gave rise to the initial water saturation and followed by the  
 180 injection of brine to recover oil; this is widely referred to as waterflooding (secondary  
 181 recovery). The latter process achieved residual oil saturation by waterflooding. Polymer and/or  
 182 nanocomposite flooding were initiated as a tertiary process (EOR) to investigate possible oil  
 183 recovery after the waterflooding process. The likely incremental oil produced will ascertain the  
 184 potential of polymer and/or nanocomposite as a viable tertiary recovery scheme. Since the  
 185 flooding experiment was not automated, monitoring of the entire sequence of operation was  
 186 done. A sampling of the effluent fluids was done every 5 minutes at the outlet of the core  
 187 holder. This is a manual process, which enabled the measurement of produced oil, and brine  
 188 for computation of core saturation and the recovery factor of the secondary and tertiary  
 189 recovery processes.

190

### 191 **3. Results and Discussion**

#### 192 *3.1 Effect of Salinity and Temperature on the Rheology of Biopolymer Nanocomposites*

##### 193 *3.1.1 Potato Peel Starch Polymer Nanocomposite (PSPNP)*

194 Biopolymer nanocomposite (PSPNP) solution (400 ppm) is made in the brine of various  
 195 salinities (28.57g/L - 2.5 wt% and 57.14g/L - 5.0 wt%) and the relationship between the  
 196 viscosity and shear rate at 50°C, 100°C, and 150°C is shown in Fig 2a-c below. Fig. 2c show  
 197 no significant effect of salinity on the viscosity of the biopolymer but exhibits shear-thinning  
 198 behaviour for all salinities. This is because of the biopolymers non-ionic nature and tolerance  
 199 of molecules. This non-ionic nature tends to improve the viscosity of the biopolymer regardless  
 200 of the salinities.

201 The PSPNP solution was heated to at varying Temperature (50°C, 100°C, 150°C) respectively.  
 202 The viscosity was measured using the viscometer. The viscosity of the PSPNP slightly declined  
 203 when temperature increased, From Fig 3a and 3b at a temperature of 50°C the viscosity of the  
 204 PSPNP was increasing and showed stability between 50°C to 120°C and degrades afterwards

205 at 150<sup>0</sup>C. The heat resistant property of PSPNP is possibly attributed to its complex structure.  
206 It did not affect the nanoparticle (Al<sub>2</sub>O<sub>3</sub>)

207

208

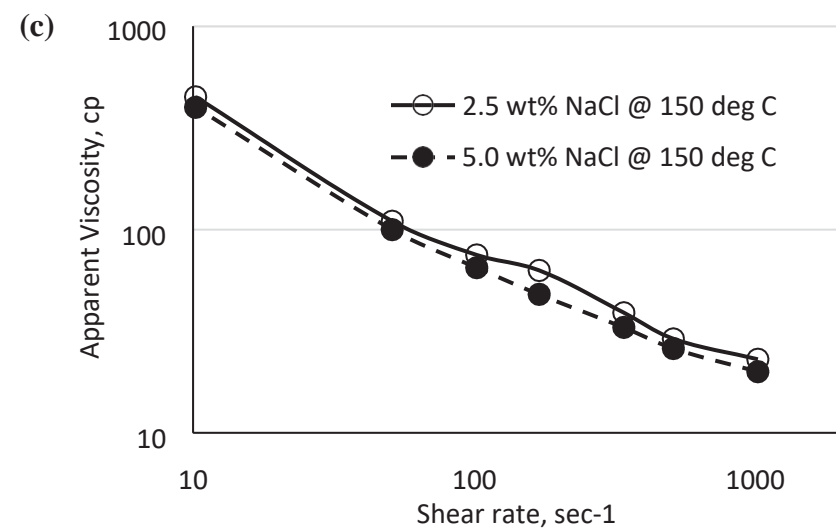
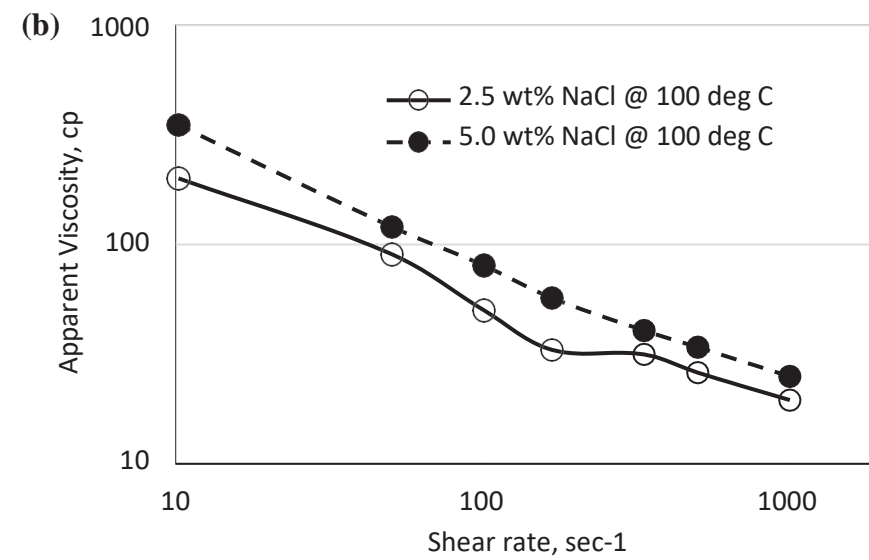
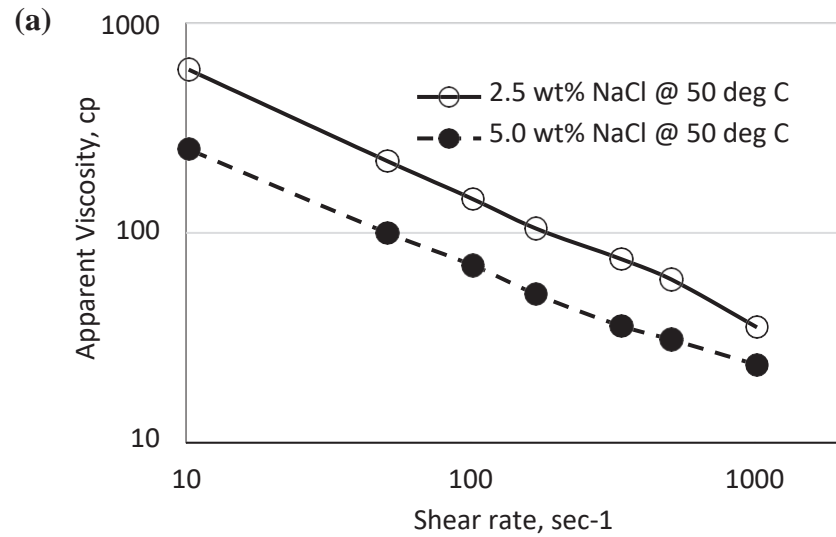
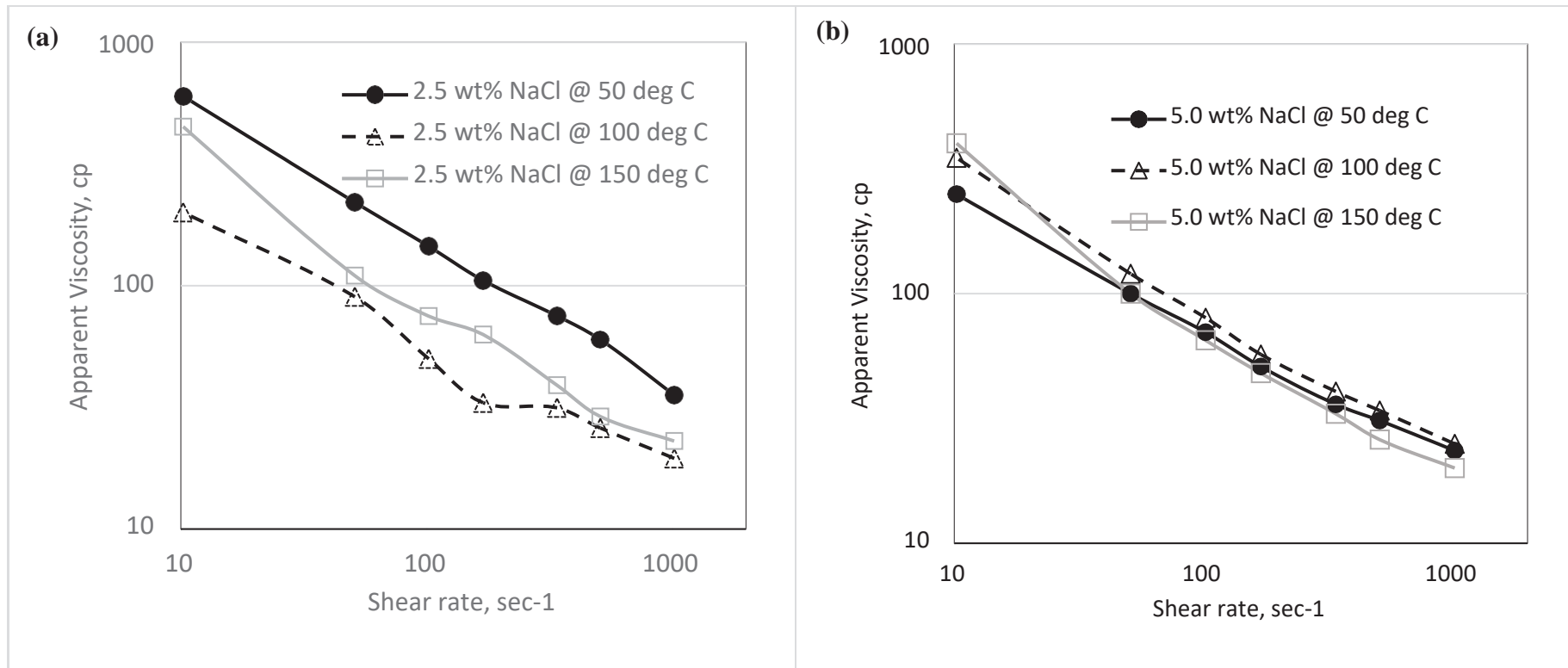


**Figure 2** – Effect of salinity (2.5 wt% and 5.0 wt%) on the apparent viscosity of the PSPNP under (a) 50°C, (b) 100°C, and (c) 150°C respectively.

209

210





211

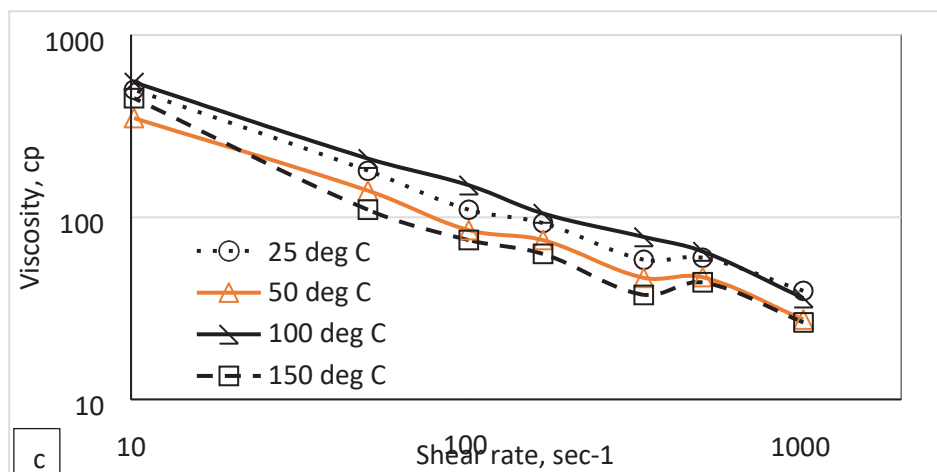
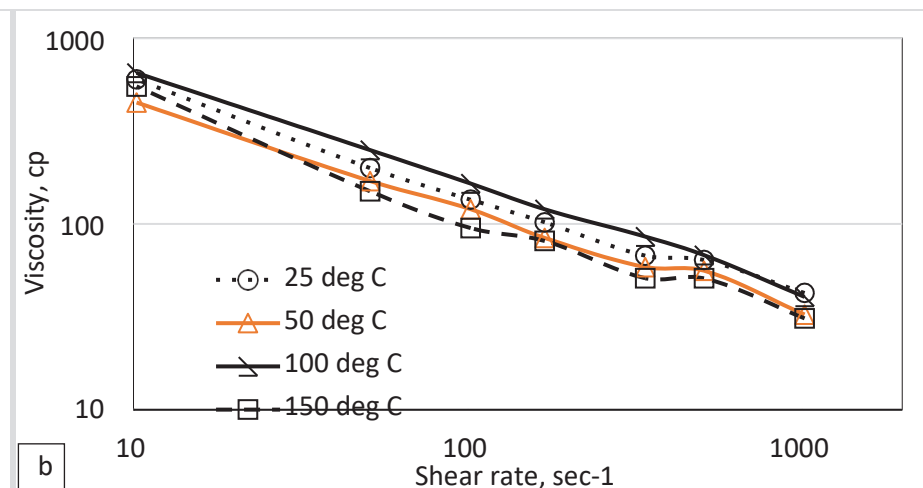
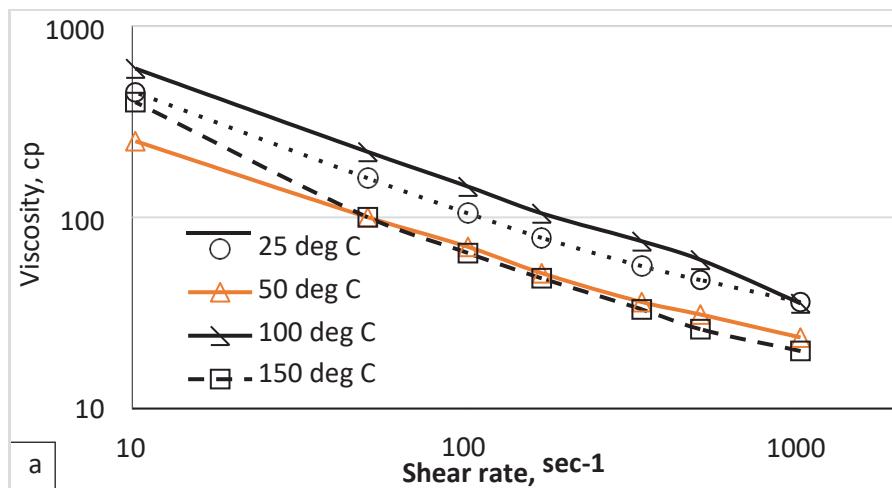
212 **Figure 3** – Effect of temperature (50°C, 100°C, and 150°C) on the apparent viscosity of the PSPNP under (a) 2.5 wt% and (b) 5.0 wt% salinity  
 213 respectively.

214 3.1.2. Gum Arabic Nanocomposite (GCNP)

215 Temperature effects on the rheology of dispersions containing Gum Arabic Nanocomposite  
216 (GCNPs) and Gum Arabic (GA) polymer showed relative stability in the viscosity of the  
217 dispersion containing GCNPs compared to GA. Also, the improvement in the rheological  
218 behaviour of the GCNPs dispersions when compared to Gum Arabic polymer could be tied to  
219 the associative interaction between polymer and nanoparticles. The associative interaction  
220 between the nanoparticle and polymer improve the gelling characteristics of the GCNPs. Figure  
221 4 displays graphically, the viscosity profile for GA and the impact of Al<sub>2</sub>O<sub>3</sub> on GA (GA  
222 nanocomposites). Furthermore, the impact of temperature at 25, 50, 100 and 150 °C on the  
223 nanocomposite is shown in Figure 5. These graphs and other accompanying dataset had earlier  
224 on been presented in Orodu *et al.* (2018a) without discussion of observed trends.

225

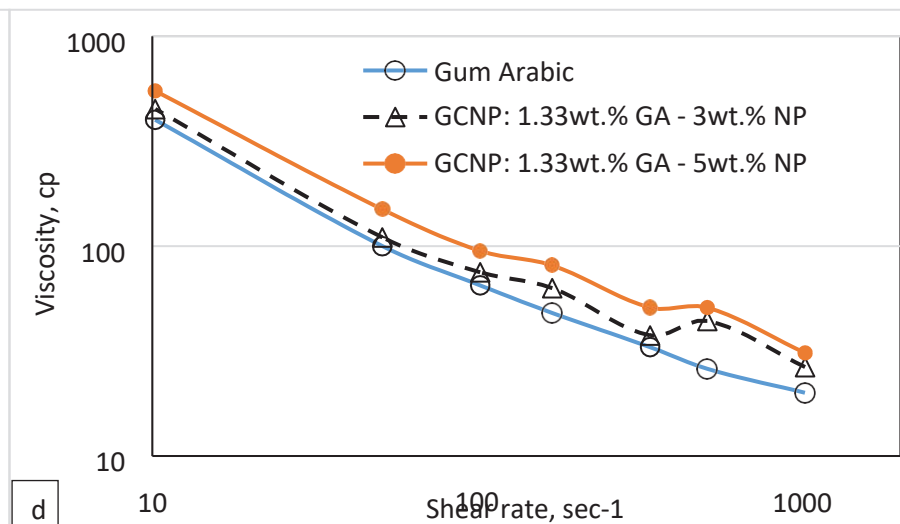
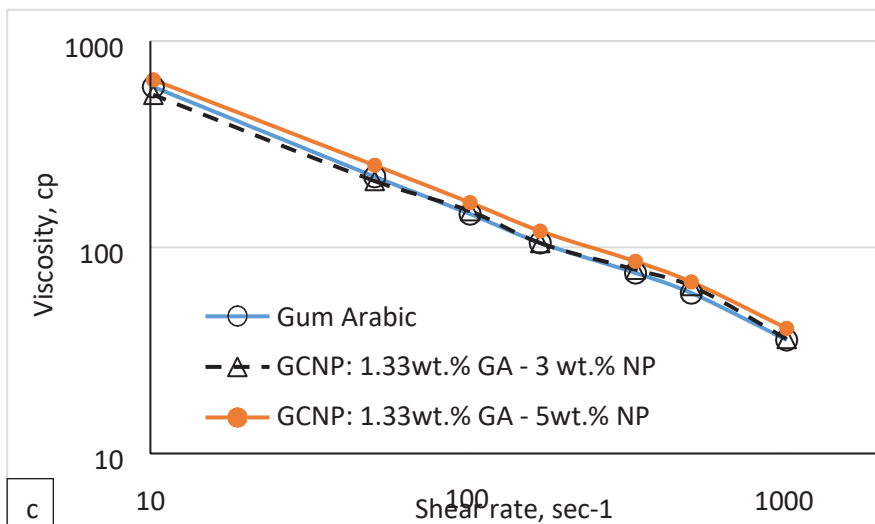
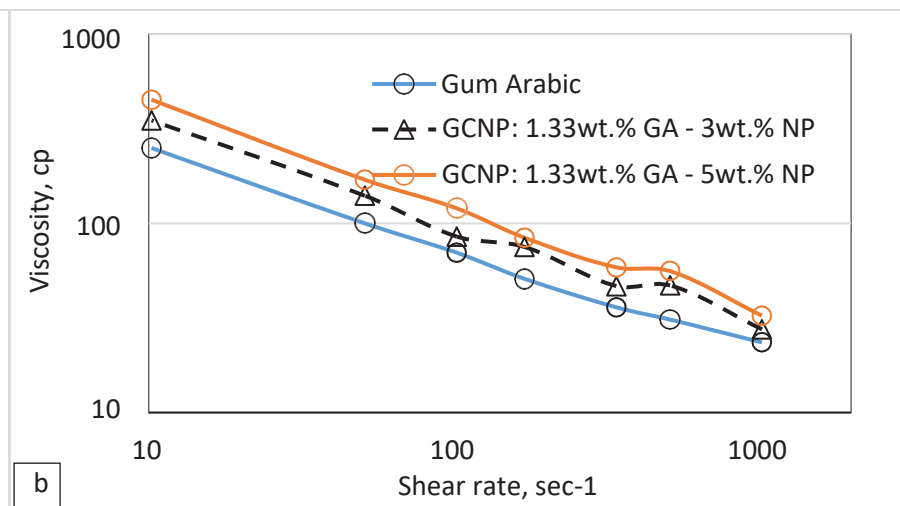
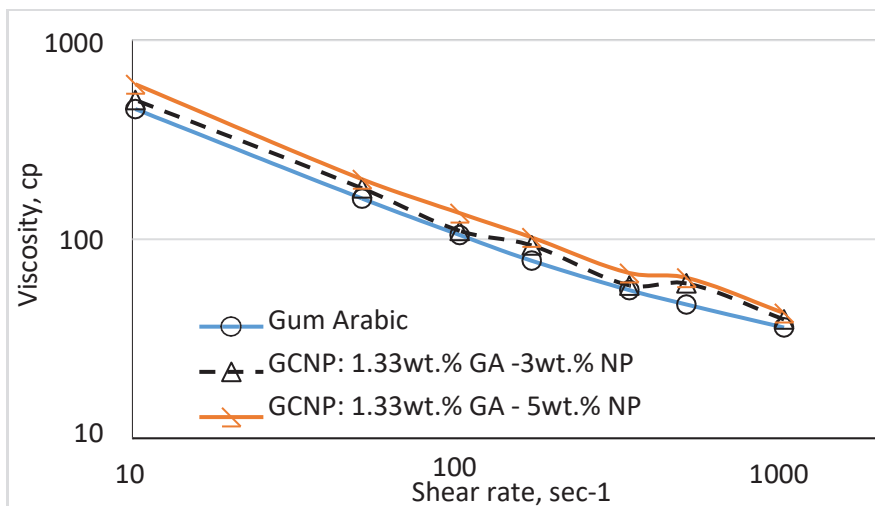
226



227

228

229 **Figure 4** - Viscosity profile for (a) GA (1.33wt.%) polymer solution (b) GCNPs (1.33wt.% GA-5wt.% Nanoparticles) (c) GCNPs (1.33wt.% GA-  
 230 5wt.% Nanoparticles (Orudu et al., 2018)



231

232

233 **Figure 5** – Gum Arabic (GA) and Gum arabic nanocomposite *viscosity profile* (a) 25 °C (b) 50 °C (c) 100 °C and (d) 150 °C (Orodu *et al.*, 2018)

234 3.2. Core flooding using Biopolymer Nanocomposite

235

236 3.2.1 Potato Peel Starch Polymer Nanocomposite (PSPNP) Coreflooding

237 The porosity and permeability estimation of core plug samples were measured using the RPT  
238 equipment. Core plugs are natural cores from the Offshore Depobelt of the Niger Delta in  
239 Nigeria. Dimensions of the cores are given in Table 2.

240

241 **Table 2 - Physical properties of Core Samples**

---

Samples	Diameter (cm)	Length (cm)	Porosity (%)	Permeability (mD)
Core B2	3.7	7	22.58	291.32
Core B3	3.7	7	26.71	293.11
Core B4	3.7	7	26.7	293.1

---

242

243 Cores B3 – B4 were subjected to secondary water flooding followed by PSP and PSPNP  
244 flooding (Figure 6) at ambient temperature and confining pressure of 200 psi. During the  
245 secondary water flooding, brine was injected into the cores to displace the oil to residual oil  
246 saturation. The biopolymer was first used to flood the core for the tertiary recovery process  
247 then after it was observed that no more oil could be recovered, then PSPNP (1.0 wt% of  
248 Nanoparticles for B3, and 1.5 wt% of Nanoparticles for B4) was used for the flooding to  
249 investigate if it could yield more recovery. For Core B3 (at an injection rate of 1.5 cc/min) oil  
250 recovery ceased, and water breakthrough commenced thereby leaving some residual oil which  
251 could still be recovered. The water flood process was able to recover about 51.13% of the  
252 OOIP. This necessitated the injection of Core B3 at additional 1.5 cc/min with PSP. The  
253 biopolymer (PSP) flooding gave a total additional recovery of 5.11 % of the total initial oil  
254 Place. The PSPNP flooding yielded a further incremental recovery of about 10.22% at an  
255 additional 2cc/min injection rate. From the flooding experiments carried out, during the PSPNP  
256 flooding for Core B3 – Core B4, it was observed that the combination of biopolymer and  
257 nanoparticles was able to recover 11.6%, and 12.43% of the OOIP (see Table 3 for a summary  
258 of the core flooding performance). This may not be unconnected with the relatively high  
259 residual oil saturation after water flooding. It is thereby indicating the capability of biopolymer  
260 nanocomposite flooding, over and above polymer flooding. It is widely known that polymer  
261 flooding serves the sole purpose of enhancing sweep efficiency by preventing the fingering of  
262 displacement fluid through oil. After the flooding process, it was observed that from the first  
263 flooding experiment to the last flooding experiment for the PSPNP (1.0 – 1.5wt% of  
264 Nanoparticles) that there was an increase in the percentage recovery of the OOIP. The increase  
265 in recovered oil stems from the increase in the concentration of nanoparticle, though marginal.  
266 The summary of the core flooding results is presented in Table 2. This includes data for Core  
267 B2 not in Figure 6. Waterflooding injection rate of 7 cc/min showed elongated and increased  
268 PV injected which led to bypass of oil but essentially recovered slightly less crude oil during  
269 waterflooding.

270

271

272 **Table 3: Core flooding parameters and result for secondary and tertiary recovery (PSP and PSPNP)**

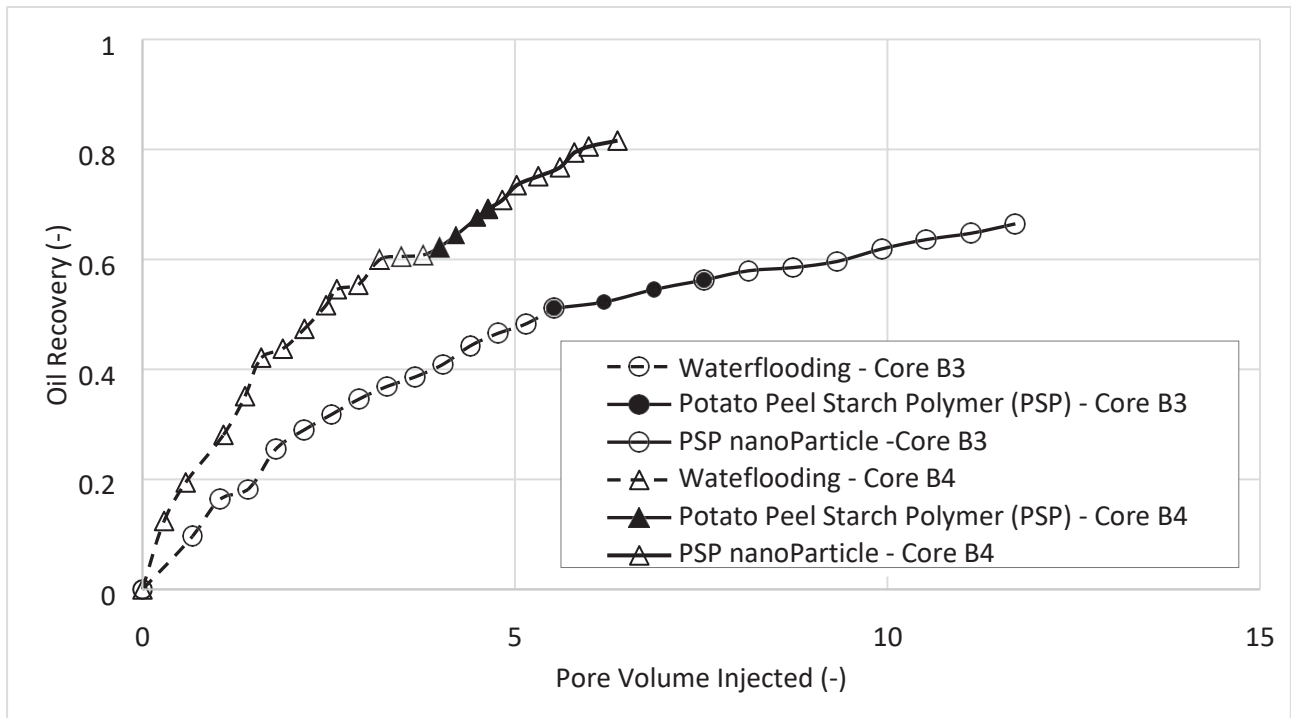
Core Sample	$S_{wi}$	Oil	$Al_2O_3$	Starch	Flooding rate (cc/min)			Residual Oil Saturation ( $S_{or}$ )			% Recovery		Total	
		API Gravity	Soln. wt%	Soln wt%	Water	PSP	PSPNP	Post Water	Post PSP	Post-PSPNP	Water	Incremental recovery		
		@ 29 °C	wt%		flooding	flooding	flooding	flooding	flooding	flooding	flooding	PSP flooding		PSPNP flooding
Core B2	0.24	34.97	0.5	5.0	7.0	1.5	2.0	0.41	0.16	0.046	51.13	5.12	10.22	64.61
Core B3	0.12	34.97	1.0	5.0	1.5	1.5	2.0	0.43	0.30	0.193	46.15	6.86	11.6	66.47
Core B4	0.12	34.97	1.5	5.0	1.5	1.5	2.0	0.34	0.19	0.065	62.16	7.02	12.44	81.62

273

274 **Table 5 – Core flooding parameters and result for secondary and tertiary recovery (GA and GCNP)**

Core Sample	$S_{wi}$	Oil	$Al_2O_3$	GA	Flooding rate (cc/min)			Residual Oil Saturation ( $S_{or}$ )			% Recovery		Total	
		API Gravity	Soln. wt%	Soln. wt%	Water	GA	GCNP	Water	GA	GCNP	Water	Incremental recovery		
		@ 29 °C	wt%		flooding	flooding	flooding	Post flooding	Post flooding	Post flooding	flooding	flooding GA		flooding GCNP
Core A	0.22	34.97	1.33	5.0	3	-	0.5	0.42	-	0.36	46.15	-	7.18	53.33
Core B	0.23	34.97	1.33	5.0	3	-	0.5	0.40	-	0.34	47.40	-	7.81	55.21
Core C	0.19	34.97	1.33	3.0	3	-	0.5	0.42	-	0.38	47.96	-	5.61	53.57
*Core D	0.19	34.97	-	3.0	3	0.5	-	0.34	0.32	-	57.89	2.63	-	60.53

275 \*After waterflooding, the core plug was flooded with Gum Arabic solution and not Gum Arabic Nanocomposite as in Core A, B, and C.



276

277 **Figure 6** – Oil Recovery after biopolymer (PSP) and biopolymer nanocomposite (PSPNP)  
 278 flooding of Core B3 – B4.

279

### 280 3.2.2 Gum Arabic Nanocomposite (GCNP) Core flooding

281 Berea sandstone cores (natural cores from the outcrop of the Berea Formation in US.)  
 282 designated as Core A, Core B, Core C and Core D were employed in the core flooding study  
 283 involving GA and GCNP at ambient temperature and confining pressure of 200 psi. Table 4  
 284 shows the properties of the cores, inclusive of the impact of GA and GCNPs flooding on  
 285 permeability impairment of the cores. The permeability reduction observed after post flooding  
 286 can be attributed to the adsorption of nanoparticles. The concentration of GCNP and Gum  
 287 Arabic are 1.33 wt.% Gum Arabic – 5.0 wt.% Al<sub>2</sub>O<sub>3</sub> Nanoparticles – GCNPs for Core-A and  
 288 Core-B, 1.33 wt.% Gum Arabic – 3.0 wt.% Al<sub>2</sub>O<sub>3</sub> Nanoparticles – GCNPs for Core-C, and  
 289 1.33 wt.% Gum Arabic for Core-D. Core D showed a minimal reduction in permeability due  
 290 to the absence of nanoparticles and permeability reduction is due to mainly polymer adsorption.  
 291 The permeability reduction is highest in cores A and B, which is flooded with GCNPs with  
 292 5wt% nanoparticles. The higher the nanoparticle content, the more the permeability impairment  
 293 observed.

294

295

296 **Table 4 - Rock Properties of the Berea cores and GCNP effect on permeability**

<b>Core Samples</b>	<b>Length (cm)</b>	<b>Diameter (cm)</b>	<b>Porosity (%)</b>	<b>Absolute Permeability</b>	<b>Permeability (GCNP flooding) (mD)</b>
Core A	6.30	3.7	18.41%	262.3	125.8
Core B	6.25	3.7	18.56%	278.8	115.4
Core C	6.30	3.7	17.89%	251.7	173.2
Core D	6.25	3.7	17.51%	245.0	223.7

297 \* Permeability of the cores as specified by Cleveland Quarries Inc. is 250mD.

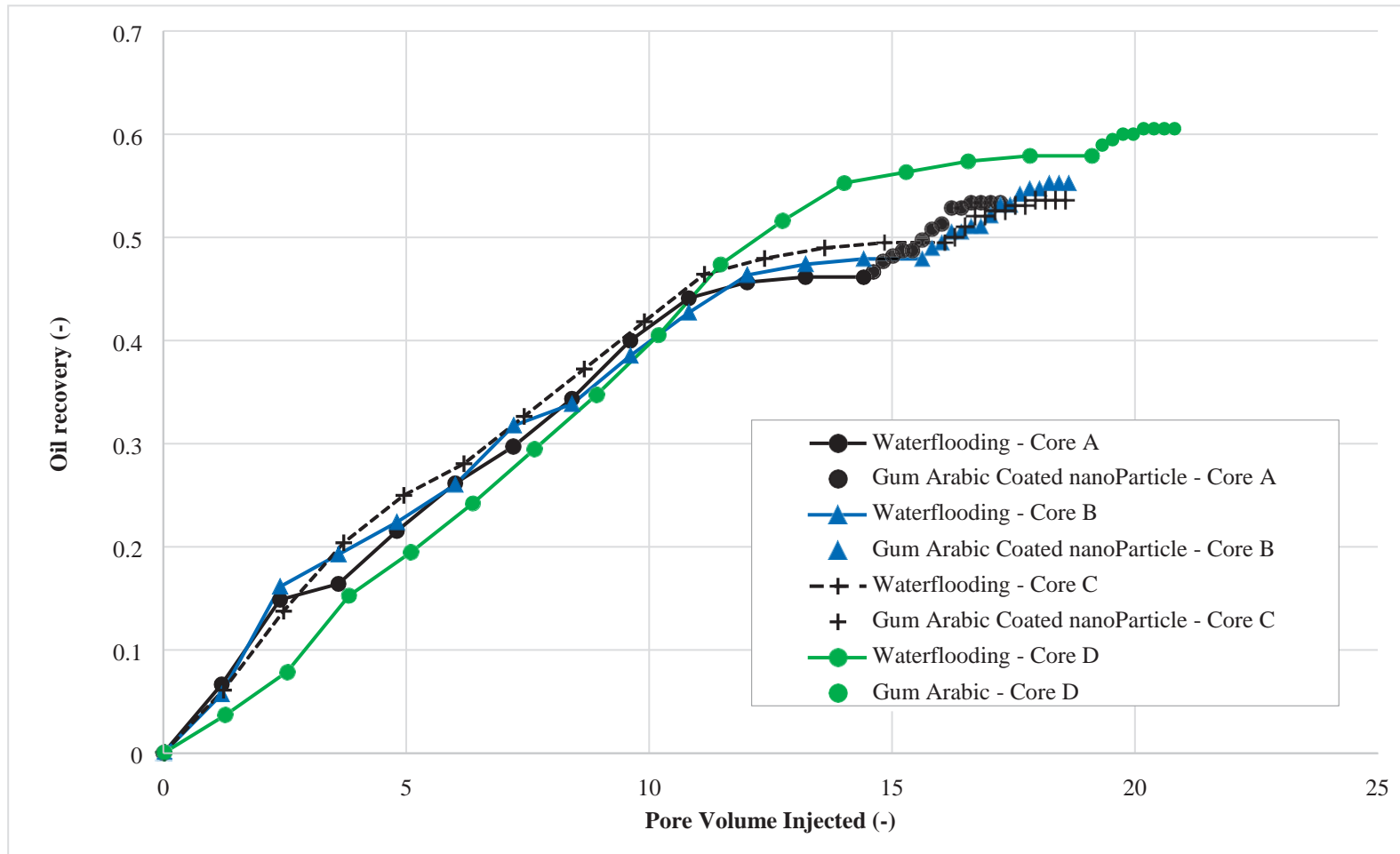
298

299 Table 5 presents a summary of results from the core flooding experiment and the associated  
300 data for the concentration of components, GA and Al<sub>2</sub>O<sub>3</sub> nanoparticles. Incremental oil  
301 recovery by EOR after waterflooding was lowest for Core-D. EOR for the core was by GA and  
302 not GCNP. The result is attributed to the higher viscosity of GCNP, hence improved mobility  
303 ratio. Besides, the impact of the Al<sub>2</sub>O<sub>3</sub> in GCNP due to the displacement mechanism at play  
304 gave rise to the enhanced incremental recovery by GCNP over GA. Graphical presentation of  
305 the performance is as viewed in Figure 7. The difference between incremental recovery for  
306 Core-A and Core-B, over Core-C, is glaring. Recovery from Core-A and Core-B is 39% and  
307 28% over Core-C. The concentration of GA used for flooding Core-A and Core-B is 5 wt%  
308 compared to 3 wt% of Core-C. Consequently, permeability reduction is higher during flooding  
309 with values of -52 %, -59%, -31 % and -9 % respectively for Core-A, Core-B, Core-C, and  
310 Core-D. These reductions in the core's permeability may be connected to the agglomeration of  
311 GA and the log-jamming effect of alumina nanoparticles at the pore-throat entrance of the  
312 porous medium of the cores.

313

315





317

318 **Figure 7** - Oil Recovery after waterflooding and gum arabic / gum arabic nanocomposite (GNCP) for Cores A, B, C and D (modified after Orodu  
 319 *et al.*, 2018b)

### 320 3.3 Discussion

321 Possible petroleum reservoir temperature range, up to the defined high-temperature limit (high-  
322 temperature range of 149 °C - 204 °C by Brujin *et al.*, 2008) was used to model experiment  
323 conducted for effect on viscosity. Hence the investigation of viscosity at 50, 100 and 150 °C.  
324 As expected, shear-thinning behaviour was observed at all fluid temperatures that were  
325 investigated. Thus, depicting non-Newtonian fluid for PSPNP and GCNP. PSPNP measured  
326 viscosity range is similar to that of Jiang *et al.* (2016). The viscosity trend at 50 °C for the salt  
327 concentration of 2.5 wt% and 5 wt% shows the same trend with that of Jiang *et al.* (2016) at a  
328 higher salt concentration. It was observed that the viscosity at 5 wt% NaCl was lower than that  
329 of 2 wt%. Jiang *et al.* (2012) stated this to be due to the reduction in interactions of the  
330 nanocomposites by the shielding effect of sodium ions. This phenomenon is asserted in Shi *et al.*  
331 *et al.* (2012) and corroborated by the electric double layer and the decrease in the Derbye's length  
332 of the nanocomposite (Shi *et al.*, 2013). However, this trend was reversed at 100 °C and  
333 maintained at 150 °C as was the case at 50 °C. Again, the effect of NaCl at 50 °C was adequately  
334 accounted for in literature. The inverse relationship of viscosity with temperature is also  
335 attributed to change from particulate network to molecular network (gel network nature)  
336 according to Herrera *et al.* (2017). This trend aligns with the reduction of hydrodynamic  
337 diameter with increasing temperature and trends in storage modulus, loss modulus and complex  
338 viscosity. The viscosity profile at 150 °C may be due to the perceived break of inter and  
339 intramolecular bonds of the nanocomposite and after that an increase of starch-water hydrogen  
340 bond (Herrera *et al.*, 2017; Shi *et al.*, 2013). In addition, cations affect the starch structure and  
341 inhibit gelatinisation temperature (Bergthaller *et al.*, 1999; Oosten, 1982). Thus, Al<sub>2</sub>O<sub>3</sub>  
342 nanoparticles affect the viscosity of PSPNP.

343 No clear explanation exists for the viscosity behaviour at 150 °C based on the knowledge of  
344 the authors. However, endothermic peak (transition) is linked to the gelatinisation of native  
345 starch that occurs within 50 to 80 °C (Herrera *et al.*, 2017; LeCorre *et al.*, 2012). One peak was  
346 observed for starch polymer but two peaks for starch-nanocrystal. The first peak for starch  
347 nanocrystal had a higher temperature and explained by the authors as due to the decline in the  
348 plasticiser, a perfect crystal and increase in crystallinity. A conclusion may be drawn for this  
349 study on the viscosity behaviour of not only PSPNP but also GCNP. Is it connected to the high  
350 energy (or temperature) to achieve endothermic transition as the case of starch? More  
351 investigation is required for this.

352 Surface-active agent of polymer-nano and emulsion formation has impacted oil recovery by  
353 further incremental recovery (Alvarez *et al.*, 2012; Foster *et al.*, 2014; Saleh *et al.*, 2005; Yoon  
354 *et al.*, 2012; Yong, 2015). Gum arabic has been known to be an active surface modifier with  
355 the formation of the stable oil-water emulsion and hence lowering IFT as widely known and  
356 stated by Gashua *et al.* (2016) and Zhang *et al.* (2007). For the emulsifying (surface-active  
357 nature) property of gum Arabic, the incremental recovery should have been higher. This brings  
358 to fore the report by Gashua (2016) on GA from Acacia senegal tree in Nigeria of the increase  
359 in hydrodynamic radius (i.e. agglomeration by electrostatic attraction) in deionised water. The  
360 solution lies in future studies by using stabilisers in preventing agglomeration like that of  
361 Gashua (2016) who used 0.5M NaNO<sub>3</sub> solution and Li *et al.* (2009) using 6M Urea. Besides,  
362 GA from Nigeria based on the samples evaluated by Gashua *et al.* (2016) forms stable oil-in-  
363 water emulsions as regards to the measurement and consistency of droplet size within a week.  
364 The investigation of IFT of gum arabic nanocomposite is essential for the knowledge on its  
365 functionality as an EOR agent with surface-active capability.

366 For the actual and fair comparison of incremental recovery from potato starch and gum arabic  
367 Al<sub>2</sub>O<sub>3</sub> nanocomposite, sand pack tube as the porous media instead core plug seems the most

368 appropriate. The aim is to guarantee relatively uniform and approximately constant porosity,  
369 permeability and sandstone grain size. Thereby enabling multiple experimental runs with only  
370 the change of sand grains at low cost. Sticking to core plugs as the test medium ensures that  
371 the experiment can be conducted under reservoir conditions. However, the evaluation of pore-  
372 throat bridging as a consequence of nanocomposite and pore throat size, and nanocomposite  
373 agglomeration is possible. Assessment through TEM/SEM and the monitoring of both the  
374 concentration of nanocomposite and core plug effluent are means of studying pore bridging  
375 and the recovery efficiency for a fair comparison of the different polymer nanocomposites.

376 Reduction in permeability during GCNP flooding is a sign of nanocomposite retention.  
377 Mechanical entrapment by the sheer size of the nanocomposite may not be the direct cause  
378 since pore-throat radius from the approximation of Winland formula (Hartmann and Coalson,  
379 1990; Martins et al., 1997) if applicable is  $\approx 11,000$  nm for the Berea cores. The  $Al_2O_3$   
380 nanoparticles size is 30 – 60 nm. Hence, the problem may be by the agglomeration of  
381 nanocomposites as earlier enumerated for gum arabic molecular association if non-swelling  
382 clay is absent in the cores. Thus, log-jamming is the primary process of nanocomposite  
383 retention.

384 Potato starch as used in this study is from the potato peel and thus ensures waste management.  
385 The availability for large scale deployment for EOR is subject for concern compared to gum  
386 Arabic. The trees, *Acacia senegal* and *Acacia seyal* from which gum Arabic comes off is  
387 formed in the wild and also cultivated. It spreads across 8000 km of the Sahel in Africa with a  
388 width of 15 km (Green Planet, 2010). This is known as the gum Arabic (or green belt) of Africa.  
389 Gashua (2016) reported the price of a tonne of raw GA as USD 1,356 in 2011. The authors of  
390 this work purchased a kg for USD 3.862 in 2017. Hence, gum arabic is readily available.  
391 Elmquist *et al.* (2005) stated that Sudan is the world's largest producer of gum arabic,  
392 accounting for 80 – 90 % of the world supply as of that time. Nigeria follows Sudan on the top  
393 producers of GA. Export from Sudan totalled up to 55,000 tonnes in 2010 (Martelli, 2010).

### 394 **Conclusion**

395 Core-flooding experiment, rheological tests were carried out to evaluate the application of  
396 biopolymer nanocomposites in enhanced oil recovery (EOR). The following conclusions are  
397 drawn from the study:

- Potato Peel Starch Nanocomposite (PSPNP) showed good viscosifying efficiency and exhibited strong shear thinning behaviour when compared to another biopolymer.
- Salinity did not show any significant effect on the biopolymer because of its non-ionic nature. The PSPNP was tested against temperature and showed stability up to 120 °C without loss of viscosity at increasing shear rate.
- Core-flooding experiment was conducted on core samples to study the recovery capability of PSPNP in porous media. The physical properties of the core samples were collected to assume a perfect reservoir condition. There was an incremental recovery from 7.02 - 12% of the initial oil in place after carrying the conventional water-flooding process.
- The PSPNP was injected to recover more oil that may have been by-passed by water-flooding giving an Incremental recovery from 2-9%. PSPNP samples produced were used in flooding cores at varying nanoparticles ( $Al_2O_3$ ) concentration (0.5wt%, 1.0wt%, 1.5wt%).
- EOR by Gum Arabic Alumina Nanocomposite showed incremental recovery from 5.16 – 7.18% over and beyond the secondary recovery scheme of waterflooding. In

addition, it was evident that the Gum Arabic nanocomposite outperformed Gum Arabic polymer flooding.

#### 412 **Acknowledgement**

413 The authors would like to thank the management of Covenant University for providing the  
414 needed facilities to carry out this research.

#### 415 **Conflict of Interest**

416 The authors have no conflict of interest to declare

417

#### 418 **Reference**

- 419 1. Abidin, A. Z., Puspasari, T., & Nugroho, W. A. (2012). Polymers for Enhanced Oil  
420 Recovery Technology. *Procedia Chemistry*, 4, 11-16.
- 421 2. Alvarez, N.J., Anna, S.L., Saigal, T., Tilton, R.D., & Walker, L.M. (2012) Interfacial  
422 dynamics and rheology of polymer-grafted nanoparticles at air-water and xylene-water  
423 inter-faces, *Langmuir*, 28:8052–63.
- 424 3. Bergthaller, W., Witt, W., & Goldau, H.P. (1999) Potato starch technology. *Stärke*  
425 (Starch), 51: 235-242.
- 430 4. Bidzinska, E., Michalec, N., Pawcencic, D. (2015) Effect of Thermal Treatment on  
431 Potato Starch Evidenced by EPR, XRD and Molecular Weight Distribution, *Magn.*  
432 *Reson. Chem.*, 53:1051-1056.92016
- 433 5. Buffo, R.A, Reineccius, G.A. & Oehlert, G.W. (2001) Factors affecting the emulsifying  
434 and rheological properties of gum *Acacia* in beverage emulsion. *Food Hydrocolloids*,  
435 **15**(1): 53–66.
- 436 6. DeBrujin G., Skeates, C., Greenaway, R., Harrison, D., Parris, M., James, S., Mueller,  
437 F., Ray, S., Riding, M., Temple, L., & Wutherich, K. (2008) High- Pressure, High –  
438 Temperature Technologies, *Schlumberger’s Oilfield Review Autumn Schlumberger*  
439 *Oilfield Review*, 20(3):46-53.
- 440 7. Degen, P., Vidoni, O. & Rehage, H. (2012) Colloid chemical properties of heat-treated  
441 gum *Acacia*. In J.F. Kennedy, G.O. Phillips and P.A Williams (Eds.), *Gum Arabic*.  
442 Special ed. Cambridge: RSC Publishing, UK, pp. 239–248
- 443 8. Elmqvist, B., Olsson, L., Elamin, E. and Warren, A. (2005) A traditional agro forestry  
444 system under threat: An analysis of gum Arabic market and cultivation in the Sudan.  
445 *Agroforestry systems*, 64: 211–218.
- 446 9. Foster, L.M., Worthen, A.J., Foster, E.L., Dong, J., Roach, C.M., Metaxas, A.E., et al.  
447 (2014) High interfacial activity of polymers “grafted through” functionalized iron oxide  
448 nanoparticle clusters, *Langmuir*, 30:10188–96
- 449 10. Gashua, I.B. (2016) An investigation of the molecular structure, composition and  
450 biophysical properties of gum Arabic, Dissertation, University of Wolverhampton, UK.
- 451 11. Gashua, I.B., Williams, P.A., & Baldwin, T.C. (2016) Molecular characteristics,  
452 association and interfacial properties of gum Arabic harvested from both *Acacia*  
453 *senegal* and *Acacia seyal*, *Food Hydrocolloids*, 61:514-522;
- 454 12. Gilbert, R.G., Gidley, M.J., Hill, S., Kilz, P., Rolland-Sabate, A., Stevenson, D.G.,  
455 Cave, R.A. (2010) Characterizing the Size and Molecular Weight Distribution of  
456 Starch: Why it is Important and Why it is Hard, *Cereal Foods World*, 55(3): 139-143.
- 457 13. Green Planet (2010). Great green wall of Africa to halt Sahara, [Online] (Accessed 21<sup>st</sup>  
458 January, 2019) Available at: < [http://www.greenplanet.com/great-green-wall-of-africa-](http://www.greenplanet.com/great-green-wall-of-africa-to-halt-sahara/)  
459 [to-halt-sahara/](http://www.greenplanet.com/great-green-wall-of-africa-to-halt-sahara/)>

- 460 14. Harding, S.E., Adams, G.G., Gillis, R.B. (2016) Molecular Weight Analysis of  
461 Starches: Which Technique, *Starch/Starke*, 68:1-8.
- 462 15. Hartmann, D. J., & Coalson, E. B. (1990) Evaluation of the Marrow Sandstone in the  
463 Sorrento Field, Cheyenne Company, Colorado, Rocky Mountain Association of  
464 Geologists, pp. 91-100.
- 465 16. Hendraningrat, L. Li, S., & Torsaeter, O. (2013a) Enhanced Oil Recovery of Low-  
466 Permeability Berea Sandstone through Optimized Nanofluids Concentration, Paper  
467 SPE 165283 presented at the SPE Enhanced Oil Recovery Conference held in Kuala  
468 Lumpur, Malaysia, 2-4 July 2013.
- 469 17. Hendraningrat, L., Li, S., & Torsaeter, O. (2013b). A Coreflood Investigation of  
470 Nanofluid Enhanced Oil Recovery. *Journal of Petroleum Science and Engineering*, 111,  
471 128-138.
- 472 18. Herrera, M.P., Vasanthan, T., & Chen, L. (2017) Rheology of starch nanoparticles as  
473 influenced by particle size, concentration and temperature, *Food Hydrocolloids*, 66:  
474 237-245.
- 475 19. Hu, Z., Haruna, M., Gao, H., Nourafkhan, E., & Wen, D. (2017.). Rheology of Partially  
476 Hydrolyzed Polyacrylamide Seeded by Nanoparticles, *Ind. Eng. Chem. Res.*, 56:3456-  
477 3463
- 478 20. Jiang, S., Liu, C., Han, Z., Xiong, L., & Sun, Q. (2016) Evaluation of rheological  
479 behavior of starch nanocrystals by acid hydrolysis and starch nanoparticles by self-  
480 assembly: A comparative study, *Food Hydrocolloids*, 52: 914-922.
- 481 21. Ju, B., Fan, T. (2009) Experimental Study and Mathematical Model of Nanoparticle  
482 Transport in Porous Media, *Powder Technology*, 192(2): 195 – 202.
- 483 22. LeCorre, D., Bras, J., & Dufrense, A. (2012) Influence of native starch's properties on  
484 starch nanocrystals thermal properties, *Carbohydrate Polymers*, 87:658-666.
- 485 23. Lewandowska K. (2006) Comparative studies of rheological properties of  
486 polyacrylamide and partially hydrolyzed polyacrylamide solutions. *J. Appl. Polym.*  
487 *Sci.*, 103: 2235–2241.
- 488 24. Li, S., Hendraningrat, L., & Torsaeter, O. (2013). Improved Oil Recovery by  
489 Hydrophilic Silica Nanoparticles Suspension: 2-Phase Flow Experiment Studies. Paper  
490 IPTC-16707 presented at the International Petroleum Technology Conference, 26-28  
491 March, Beijing, China.
- 492 25. Li, X., Fang, Y., Al-Assaf, S., Phillips, G.O., Nishinari, K. & Zhang, H. (2009)  
493 Rheological study of gum Arabic solutions: Interpretation based on molecular self-  
494 association. *Food Hydrocolloids*, **23**: 2394–2402.
- 495 26. Maghzi, A, Mohammadi, S., Ghazanfari, M.H., Kharrat, R. Masihi, M. (2012)  
496 Monitoring Wettability Alteration by Silica Nanoparticles during Water Flooding to  
497 Heavy Oils in Five-Spot Systems: A Pore-Level Investigation. *Experimental Thermal*  
498 *and Fluid Science* 40 (2012): 168-176.
- 499 27. Mahendran, T., Williams, P.A., Phillips, G.O., Al-Assaf, S. & Baldwin, T.C. (2008)  
500 New insights into the structural characteristics of the arabinogalactan–protein (AGP)  
501 fraction of gum Arabic. *J. Agric. Food Chem.*, **56**: 9269–9276.
- 502 28. Martin, A. J., Solomon, S. T., & Hartmann, D.J. (1997) Characterization of  
503 petrophysical flow units in carbonate reservoirs, *AAPG Bulletin*, 81(5): 734-759.
- 504 29. Mauryu, N.K., Kushwaha, P., Mandal, A. (2017) Studies on Interfacial and Rheological  
505 Properties of Water Soluble Polymer Grafted Nanoparticle for Application in Enhanced  
506 Oil Recovery, *Journal of Taiwan Institute of Chemical Engineers*, 70:319 – 330.
- 507 30. Mertelli, S. (2011) Gum arabic a potential cure for sudanese ill., [Online] (Accessed  
508 22<sup>nd</sup> January, 2019) Available at: [https://phys.org/news/2011-11-gum-arabic-potential-](https://phys.org/news/2011-11-gum-arabic-potential-sudanese-ills.html)  
509 [sudanese-ills.html](https://phys.org/news/2011-11-gum-arabic-potential-sudanese-ills.html)

- 510 31. Ogolo, N. A., Olafuyi, O. A., & Onyekonwu, M. O. (2012). Enhanced Oil Recovery  
511 Using Nanoparticles. *SPE Saudi Arabia Section Technical Symposium and Exhibition*  
512 (pp. 1-9). Al-Khobar: Society of Petroleum Engineers.
- 513 32. Oosten, B.J. (1982) Tentative hypothesis to explain how electrolytes affect the  
514 gelatinization temperature of starches in water. *Stärke (Starch)*, 34: 233-239.
- 515 33. Orodu, O.D., Orodu, K.B., Afolabi, R.O., Eboh, D.A. (2018a) Rheology of Gum Arabic  
516 Polymer and Gum Arabic Coated Nanoparticle for Enhanced Recovery of Nigerian  
517 Medium Crude Oil under Varying Temperatures, *Data in Brief*. 19(2018): 1773-1778.
- 518 34. Orodu, O.D., Orodu, K.B., Afolabi, R.O., Eboh, D.A. (2018b) Dataset on Experimental  
519 Investigation of Gum Arabic Coated Alumina Nanoparticles for Enhanced Recovery of  
520 Nigerian Medium Crude Oil, *Data in Brief*. 19:475-480.
- 521 35. Osamah, A. A., Khaled, M. M., & Yousef, A. H. (2015). Experimental study of  
522 Enhanced-Heavy-Oil Recovery in Berea Sandstone Cores by Use of Nanofluids  
523 Applications. *SPE Reservoir Evaluation & Engineering* 18(3), 1-13.
- 524 36. Pittman, E. D. (1992) Relationship of Porosity and Permeability to Various Parameters  
525 Derived from Mercury Injection-Capillary Pressure Curves for Sandstone. *AAPG*  
526 *Bulletin* 76(2):191-198.
- 527 37. Renard, D., Lavenant-Gourgeon, L., Ralet, M.C. and Sanchez, C. (2006) *Acacia*  
528 *senegal* gum: continuum of molecular species differing by their protein to sugar ratio,  
529 molecular weight, and charges. *Biomacromolecules*, 8, pp. 2637–2649
- 530 38. Rodriguez, E., Roberts, M. R., Yu, H., Huh, C., & Bryant, S. L. (2009) Enhanced  
531 Migration of Surface-Treated Nanoparticles in Sedimentary Rocks, SPE 124418  
532 presented at the 2009 SPE Annual Technical Conference and Exhibition, New Orleans,  
533 LA, 4-7 October.
- 534 39. Roustaei, A., Moghadasi, J., Bagherzadeh, H., & Shahrabadi, A. (2012). An  
535 Experimental Investigation of Polysilicon Nanoparticles' Recovery Efficiencies  
536 through Changes in Interfacial Tension and Wettability Alteration. SPE Paper 156976  
537 presented at the SPE International Oilfield Nanotechnology Conference and Exhibition,  
538 12-14 June, Noordwijk, The Netherlands.
- 539 40. Saha, R., Ramgopal, V. S., & Tiwari, P. (2018). Silica Nanoparticle Assisted Polymer  
540 Flooding of Heavy Crude Oil: Emulsification, Rheology, and Wettability Alteration  
541 Characteristics. *Industrial and Engineering Chemistry Research*, 57, 6364-6376.
- 542 41. Saleh, N., Sarbu, T., Sirk, K., Lowry, G.V., Matyjaszewski, K., & Tilton, R.D. (2005)  
543 Oil-in-water emulsions stabilized by highly charged polyelectrolyte-grafted silica  
544 nanoparticles. *Langmuir*, 21:9873–8
- 545 42. ShamsiJazeyi, H., Miller, C. A., Wong, M. S., Tour, J. M., & Verduzco, R. (2014).  
546 Polymer-Coated Nanoparticles for Enhanced Oil Recovery. *Journal of Applied*  
547 *Polymer Science*, 131(15), 1-13.
- 548 43. Sharma, T., Sanwai, J.S. (2017) Silica Nanofluids in Polyacrylamide with and without  
549 Surfactant: Viscosity, Surface Tension, and Interfacial Tension with Liquid Paraffin,  
550 *Journal of Petroleum Science and Engineering*, 152: 575 – 585.
- 551 44. Shi, A.M., Li, D., Wang, L., & Adhikari, B. (2012) The effect of NaCl on the  
552 rheological properties of suspension containing spray dried starch nanoparticles,  
553 *Carbohydrate Polymers*, 90: 1530-1537.
- 554 45. Shi, A.M., Li, D., Wang, L., & Adhikari, B. (2013) Suspension of vacuum-freeze dried  
555 starch nanoparticles: Influence of NaCl on their rheological properties, *Carbohydrate*  
556 *Polymers*, 44:782-790.
- 557 46. Sun, X., Zhang, Y., Chen, G., & Gai, Z. (2017) Application of Nanoparticles in  
558 Enhanced Oil Recovery: A Critical Review of Recent Progress, *Energies* 10(3): 345

- 559 47. Taiwo, O., Olafuyi, O.A. (2015) Surfactant and Surfactant-polymer Flooding for Light  
560 Oil: A Gum Arabic Approach, *Petroleum and Coal*, 57(3): 205 –215.
- 561 48. Tan, C.T. (2004) Beverage emulsions. In Frieberg, S.E., Larsson, K. and Sjoblom, J.  
562 (eds.) *Food Emulsions*. 4th ed. CRC Press: Boca, pp. 485–524.
- 563 49. Yong, X. (2015) Modeling the assembly of polymer-grafted nanoparticles at oil–water  
564 interfaces. *Langmuir*, 31:11458–69.
- 565 50. Yoon, K.Y., Li, Z., Neilson, B.M., Lee, W., Huh, C., Bryant, S.L., et al. (2012) Effect  
566 of adsorbed amphiphilic copolymers on the interfacial activity of superparamagnetic  
567 nanoclusters and the emulsification of oil in water. *Macromolecules*, 45:5156–7.
- 568 51. Yousefvand, H., & Jafari, A. (2015). Enhanced Oil Recovery using Polymer/nanosilica.  
569 *Procedia Material Science*, 565-570.
- 570 52. Yu, J., Berlin, J. M., Lu, W., Zhang, L., Kan, A. T., Zhang, P., . . . Tomson, M. B.  
571 (2010). Transport Study of Nanoparticles for Oil Field Application. *SPE International*  
572 *Conference on Oilfield Scale* (pp. 1-16). Aberdeen: Society of Petroleum Engineers.
- 573 53. Zhang, H., Shan, G., Liu, H., & Xing, J. (2007) Surface Modification of  $\gamma$ -Al<sub>2</sub>O<sub>3</sub> Nano-  
574 particles with Gum Arabic and its Applications in Adsorption and Biodesulfurization,  
575 *Surface and Coatings Technology*, 201:6917-6921.

576